Low-Temperature High-Efficiency Preparation of TiB₂ Micro-Platelets *via* Boro/Carbothermal Reduction in Microwave Heated Molten Salt

Jie Liu, Jianghao Liu *, Yuan Zeng, Haijun Zhang * and Zhi Li

The State Key Laboratory of Refractories and Metallurgy, Wuhan University of Science and Technology, Wuhan 430081, China
* Correspondence: liujianghao2014@wust.edu.cn (J.L.); zhanghaijun@wust.edu.cn (H.Z.)

check for updates

Abstract: A molten-salt and microwave co-facilitated boro/carbothermal reduction methodology was developed for low temperature high-efficiency synthesis of TiB₂ powders. By using relatively inexpensive titanium oxide (TiO_2), boron carbide (B_4C) and amorphous carbon (C) as raw materials, single-phase TiB₂ powders were prepared after 60 min at as low as 1150 °C or after only 20 min at 1200 °C. Such synthesis conditions were remarkably milder than those required by the conventional reduction routes using the identical reducing agent. As-synthesized TiB₂ powders exhibited single-crystalline nature and well-grown hexagonal-platelet-like morphology. The achievement of low temperature high-efficiency preparation of high-quality TiB₂ microplatelets in the present work was mainly attributable to the synergistic effects of molten-salt medium and microwave heating.

Keywords: TiB₂; hexagonal microplatelet; microwave heating; molten-salt synthesis

1. Introduction

As one of the most important ultra-high temperature ceramics (UHTCs), titanium diboride (TiB₂) exhibits many useful properties, including a high melting point (3225 °C), low density (4.52 g·cm⁻³), good corrosion resistance, and high hardness (25–35 GPa) [1–4]. It is thus regarded as a candidate material that is potentially applicable to versatile structural-applications, e.g., in armors, high-temperature wear-resistant parts, cutting tools, and neutron absorbers [5–7]. Currently, the most popular method to prepare TiB₂-based UHTCs is high temperature consolidation of constituent powders, in which case the synthesis process and the quality of raw material powders (in particular, TiB₂ powder) are key in optimization of the properties and performance of the final products.

The main synthesis techniques of TiB₂ powders developed to date can be categorized into three types, including self-propagating high-temperature synthesis (SHS) [8], carbo/boro/metallothermic reduction [9–21] and sol-gel processing [22,23]. Owing to its relatively low material cost and good processing controllability, the reduction methodology has been and is still being used extensively. For instance, Moradi et al. [13] synthesized TiB₂ powders from TiO_2, B_2O_3 and graphite *via* carbothermal reduction at 1380 °C for 60 min. Yu et al. [12] prepared TiB₂ powders by firing powder mixtures of TiO_2, B_4C and carbon black at 1600 °C for 30 min. Nevertheless, it is still a great challenge to moderate the synthesis conditions of TiB₂ and the overall production cost.

To address the aforementioned issues, several advanced strategies, e.g., molten-salt medium and microwave heating, were employed to modify the conventional boro/carbothermal reduction method (BCTR) in the synthesis of TiB₂ [14,24]. As is well documented [17,18], molten-salt, as a liquid medium, exhibits several important merits in materials synthesis. Apart from reducing the synthesis temperature and accelerating the reaction process, it facilitates diffusive mass transfer and self-assembly processes

and thus the formation of highly-crystalline product with intrinsically-anisotropic morphology [25]. On the other hand, microwave heating is capable of selectively heating the material with good microwave absorbability, thus additionally reducing the synthesis temperature and significantly accelerating the overall reaction process. More importantly, it is also effective in inducing the nucleation and therefore accelerating the growth process and enhancing the crystalline degree of synthesized crystals [26–28]. Consequently, the introduction of molten-salt medium combined with microwave heating showed crucial positive effects on the overall synthesis process, as well as on the crystalline degree and morphology of the powder product [29,30].

In this work, such a molten-salt and microwave heating co-facilitated boro/carbothermal reduction method (MSM-BCTR), was adopted to prepare TiB_2 powders with high crystalline degree and anisotropic morphology by using inexpensive TiO_2, B_4C and amorphous C as raw materials, while avoiding using any costly B or active metal (Mg or Al) reducing agents. The influence of processing parameters including temperature, dwelling time, microwave/salt medium conditions and the amount of reducing agent on the phase composition and microstructure of powder product was systematically investigated, so as to confirm the superiority of MSM-BCTR over the conventional methods in the preparation of high-quality TiB_2 powders as well as a broad range of UHTCs.

2. Experimental Procedures

2.1. Raw Materials

Amorphous carbon was purchased from Sinopharm chem. Co. Ltd (Shanghai, China), boron carbide (B_4C, purity > 95.0 wt%) was purchased from Mudanjiang Jingangzuan Boron-Carbide Co. Ltd. (Mudanjiang, China). titanium oxide (TiO_2, rutile phase, purity > 99.9 wt%), sodium chloride (NaCl, purity > 99.9 wt%) and potassium chloride (KCl, purity > 99.9 wt%) were purchased from Bodi Chem. Co. Ltd. (Tianjin, China).

$$2TiO_2(s) + B_4C(s) + 3C(s) = 2TiB_2(s) + 4CO(g) \qquad (1)$$
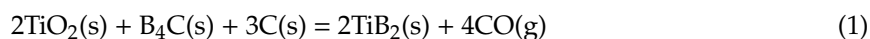
B_4C took part in the overall synthesis reaction (Reaction 1), as both boron source and reducing agent. To compensate for the volatilization loss of boron species at high temperature [30], the amount of B_4C was slightly higher than the stoichiometric amount indicated by Reaction 1. To minimize the residual carbon in the final powder product, the stoichiometric amount of carbon was used in all the cases. The batch compositions, along with processing conditions, are listed in Table 1.

Table 1. Batch Compositions and Processing Parameters for Manufacturing TiB_2 Powders by the MSM-BCTR method.

Sample No.	Molar Ratio			Heating Mode	Temperature (°C)	Dwelling Time (min)	Salt Medium
	TiO_2	B_4C	C				
MSMBC-1	1.0	0.8	1.5	MWH †	1150	20	NaCl/KCl
MSMBC-2	1.0	0.8	1.5	MWH	1150	60	NaCl/KCl
MSMBC-3	1.0	0.8	1.5	MWH	1200	0	NaCl/KCl
MSMBC-4	1.0	0.8	1.5	MWH	1200	20	NaCl/KCl
MSMBC-5	1.0	0.8	1.5	CH†	1200	20	NaCl/KCl
MSMBC-6	1.0	0.8	1.5	MWH	1200	20	–
MSMBC-7	1.0	0.7	1.5	MWH	1200	20	NaCl/KCl

† MWH and CH denote microwave heating and conventional heating, respectively.

2.2. Methodologies

The reactants and salts (NaCl/KCl) in a weight ratio of 1:2 were mixed manually and then contained in a crucible of 10 mm in diameter and 15 mm in height. The crucible was placed in a columnar saggar, which was subsequently positioned in a microwave furnace (HAMiLab-V3000, Changsha Longtech Co.

Ltd. Changsha, China) protected by flowing argon atmosphere. Green silicon carbide (SiC) powder was used to fill the free space of saggar to assist with microwave heating of the powder mixture. The furnace temperature was monitored by an infrared thermometer (Yongtai, Xi'an, China). In a typical MSM-BCTR process, the furnace was firstly heated at a constant rate of 10 °C/min to a pre-determined temperature within 1150–1200 °C, and then held for 0–60 min before cooling naturally to the ambient temperature. The reacted powders were repeatedly rinsed with hot deionized water (80 °C) to remove the residual salt, followed by overnight drying in a vacuum oven at 80 °C.

Phases in raw materials and product samples were analyzed by an X-ray diffractometer (XRD, PANalytical, Hillsboro, The Netherlands) with CuK_{α} radiation (λ = 0.1542 nm) at a scan rate of 5°(2θ)/min. ICDD cards of No.00-035-0741, No.03-065-8805, No.03-035-0798 and No.03-065-1118 were used to identify the crystallographic phases of TiB_2, TiC, B_4C and TiO_2, respectively. Morphologies and sizes of TiB_2 product powders were examined using a field-emission scanning electron microscope (FE-SEM, 15 kV, Nova400NanoSEM, PHILIPS, Amsterdam, The Netherlands) equipped with an energy dispersive spectrometer (EDS, IET 200, Oxford, UK), and a transmission electron microscope (TEM, 200 kV, JEM-2100UHRSTEM, JEOL, Tokyo, Japan). For TEM characterization, the as-obtained powders were firstly ultrasonically dispersed in ethanol for 30 min, followed by natural seasoning in the air.

3. Results and Discussion

Figure 1 presents X-ray diffraction (XRD) patterns of samples prepared by MSM-BCTR at 1150 °C for 20 and 60 min, respectively. In the case of 20 min (sample MSMBC-1), only TiB_2 and TiC (formed respectively from Reaction 1 and Reaction 2) but no other phases were detected, indicating the complete reduction of the TiO_2 precursor *via* Reaction 2 and incompletion of Reaction 3. Interestingly, upon just extending the dwelling time at 1150 °C from 20 to 60 min, TiC disappeared and only TiB_2 was formed (sample MSMBC-2), indicating the high efficiency of the conversion reaction from TiC to TiB_2 (Reaction 3), and the completion of the overall reaction (Reaction 1) after a short time period at such a low firing temperature.

$$TiO_2(s) + 3C(s) = TiC(s) + 2CO(g) \tag{2}$$

$$2TiC(s) + B_4C(s) = 2TiB_2(s) + 3C(s) \tag{3}$$
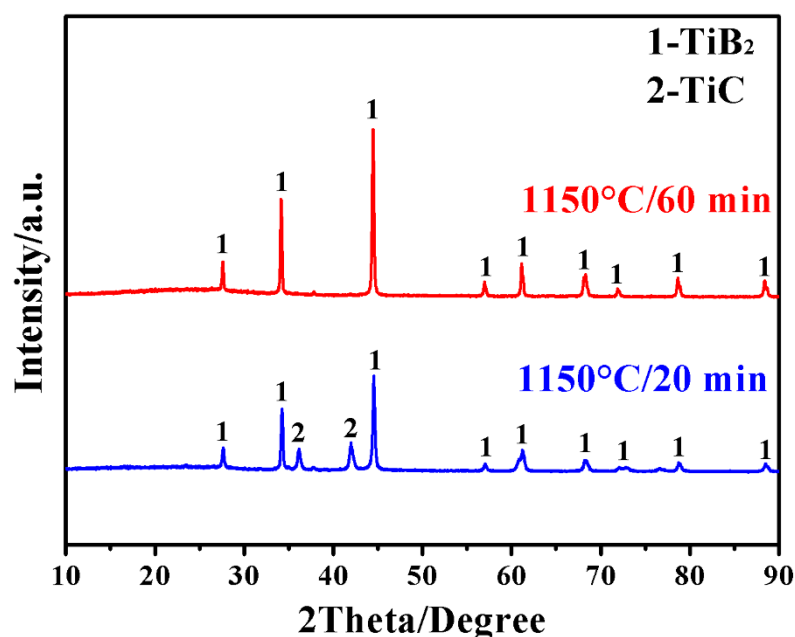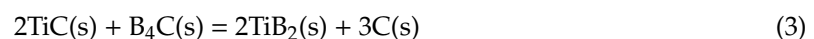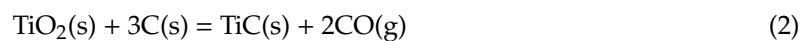
Figure 1. Phase formation in samples prepared by MSM-BCTR at 1150 °C for respectively 20 and 60 min.

Figure 2 further shows XRD patterns of samples after MSM-BCTR at a slightly higher temperature of 1200 °C. In the case of zero dwelling time (sample MSMBC-3), TiB_2 was already formed as the main crystalline phase, although certain amounts of reactants (TiO_2 and B_4C) still remained along with minor intermediate phase of TiC. Despite this, upon slightly extending the dwelling time to 20 min (sample MSMBC-4), other than the desired TiB_2, all other impurity phases disappeared completely. Comparing Figure 1 with Figure 2 suggests that such a small enhancement in firing temperature was effective in accelerating not only the direct formation of TiB_2 but also the conversion from TiC to TiB_2 (Reactions 1–3). It was worth noting that the synthesis conditions (1150 °C/60 min and 1200 °C/20 min) in the present work were considerably milder than in the cases of conventional BCTR (up to 1600 °C for several hours) using the identical type of reducing agent [12], and the molten-salt-solely-assisted BCTR (firing temperature of 1000 °C and dwelling time of 4 h) using even much more expensive magnesium (Mg) as a reducing agent [16]. These results demonstrated that the present MSM-BCTR method was promising for low-cost, energy-saving, and high-efficiency preparation of TiB_2 powders, which should be attributed to the combined effect of molten-salt medium and microwave heating, as described in the "Introduction" section and discussed in our previous papers [29,30].
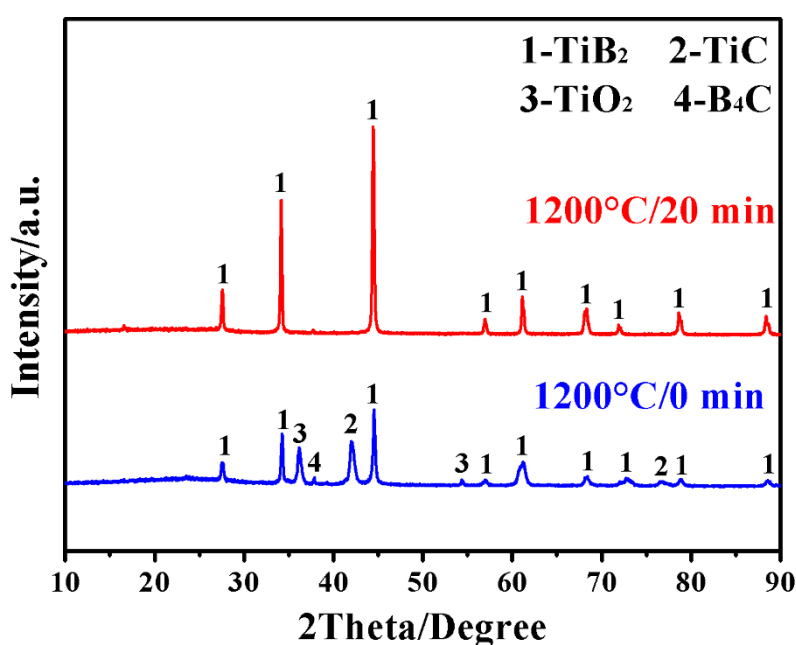
Figure 2. Phase formation in samples after MSM-BCTR treatments at 1200 °C for 0 and 20 min, respectively.

For comparison and further confirming the effectiveness of microwave heating and molten-salt medium on the synthesis of TiB_2, samples with the same batch compositions were also fired at as-optimized temperature conditions (1200 °C/20 min), using solely microwave heating or salt medium. As shown in Figure 3, in the case without using microwave (sample MSMBC-5), TiO_2 remained as the dominant phase and no TiB_2 was detected, indicating the crucial role played by microwave heating in the TiB_2 formation (*via* Reaction 1–3). On the other hand, due to microwave-assisted BCTR under identical processing conditions, the XRD pattern of sample (sample MSMBC-6) shows the peaks of TiB_2, B_4C and $TiBO_3$, in which the intensities of TiB_2 peaks were obviously higher than that of others, indicating the higher crystallization degree of the TiB_2 phase. Apart from TiB_2, un-reacted B_4C were still present along with the intermediate phase of $TiBO_3$ which was formed *via* Reaction 4 but tended to be further converted into TiB_2 (*via* Reaction 5) [13]. The above comparison verified the respective role played by microwave heating and molten-salt medium in the low-temperature rapid synthesis of TiB_2.

$$2TiO_2(s) + B_2O_3(g) + C(s) = 2TiBO_3(s) + CO(g) \tag{4}$$

$$2TiBO_3(s) + B_2O_3(g) + 9C(s) = 2TiB_2(s) + 9CO(g) \tag{5}$$
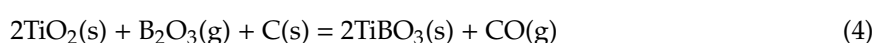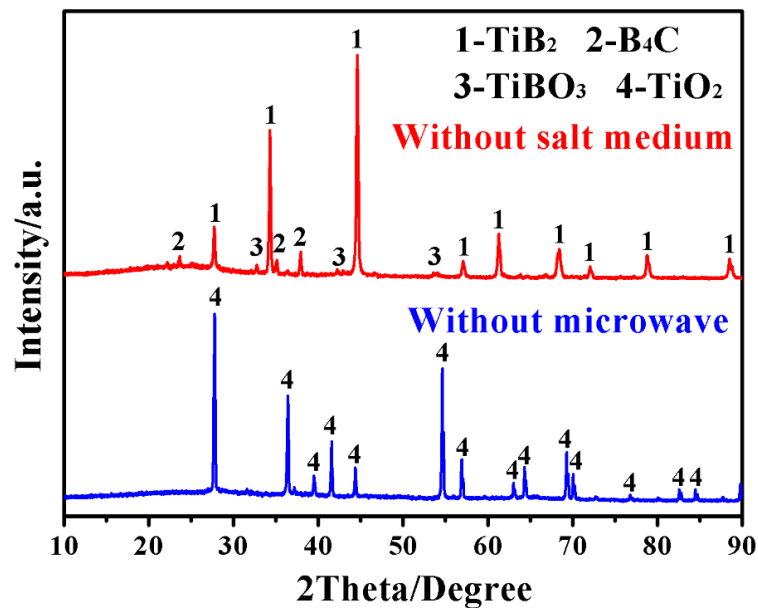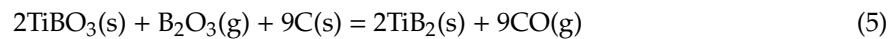
Figure 3. Phase formation in MSM-BCTR samples resultant from 20 min firing at 1200 °C, using solely microwave heating or molten-salt medium.

In addition to firing temperature and dwelling time, the amount of B_4C significantly affected the synthesis process and the quality of the product powder. Specifically, the use of inadequate amount of B_4C would hinder the desirable reduction reaction due to lack of reducing atmosphere, whereas the use of excessive B_4C would leave high levels of impurities (mainly amorphous C), seriously deteriorating the purity and sinterability of the product powder [9]. Figure 4, as an example, compares phase compositions and reaction extents of the samples initially containing respectively 60 mol% and 40 mol% excess B_4C, after 20 min MSM-BCTR at 1200 °C. In the case of the former (MSMBC-4), apart from TiB_2, neither the residual reducing agent nor an impurity phase was detected. However, in the case of the latter (MSMBC-7), despite the presence of the main phase of TiB_2 and the absence of reducing agent, two diffraction peaks of TiO_2 with low intensities were still visible, which demonstrated the importance of using appropriately excess amount of reducing agent for ensuring the overall synthetic reactions (Reactions 1–3) to go to completion. It should be noted that, in this process, the requirement of excess boron source was mainly attributable to the evaporation loss of the intermediate product of B_2O_3. Specifically, owing to its low melting point and high volatility, B_2O_3, as the product of borothermal reduction reaction (Reaction 6) would suffer from significant evaporation loss even at a low temperature range of 900–1100 °C, thus resulting in incompletion of the subsequent carbothermal reduction reaction (Reaction 7) for synthesizing TiB_2 [21]. Based on the comparison result, it could be concluded that, under the present MSM-BCTR conditions, 60 mol% excessive B_4C should be used for synthesizing phase pure TiB_2 powder.

$$7TiO_2(s) + 5B_4C(s) = 7TiB_2(s) + 3B_2O_3(s) + 5CO(g) \tag{6}$$

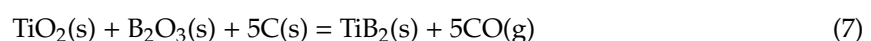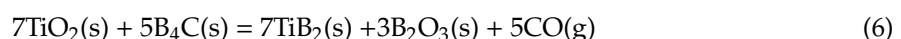$$TiO_2(s) + B_2O_3(s) + 5C(s) = TiB_2(s) + 5CO(g) \tag{7}$$

Figure 5 shows microstructure and phase morphology of MSMBC-4, along with the corresponding EDS results. A small amount of monodispersed well-defined hexagonal microplatelets (Figure 5a) coexisted with a large quantity of agglomerates comprising dozens of interlaced micro-platelets (Figure 5b). The corresponding EDS results (presented in Figure 5c–f) revealed that only Ti and B were detected

and homogeneously distributed in the microplatelets, confirming that they were TiB_2. Moreover, except for TiB_2, no impurity phases (TiO_2, B_4C and carbon) were detected, further confirming the high purity of the microplatelets. And the highly-crystallized hexagonal TiB_2 micro-platelets generally had micron-scale lengths (average length of 4.2 µm) and submicron-scale thicknesses (average thickness of 0.6 µm) with narrow size distributions. Such well-grown hexagonal TiB_2 microplatelets looked similar to those formed *via* the conventional reduction routes using the identical raw materials, but the synthesis conditions in the case of the latter were much harsher (1600 °C/30 min) [12].
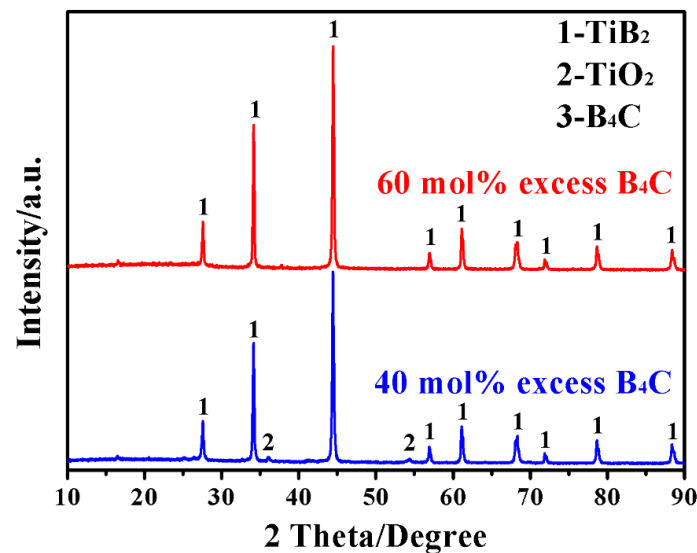
**Figure 4.** XRD patterns of samples containing initially 40 and 60 mol% excessive B_4C, after MSM-BCTR treatments at 1200 °C for 20 min.
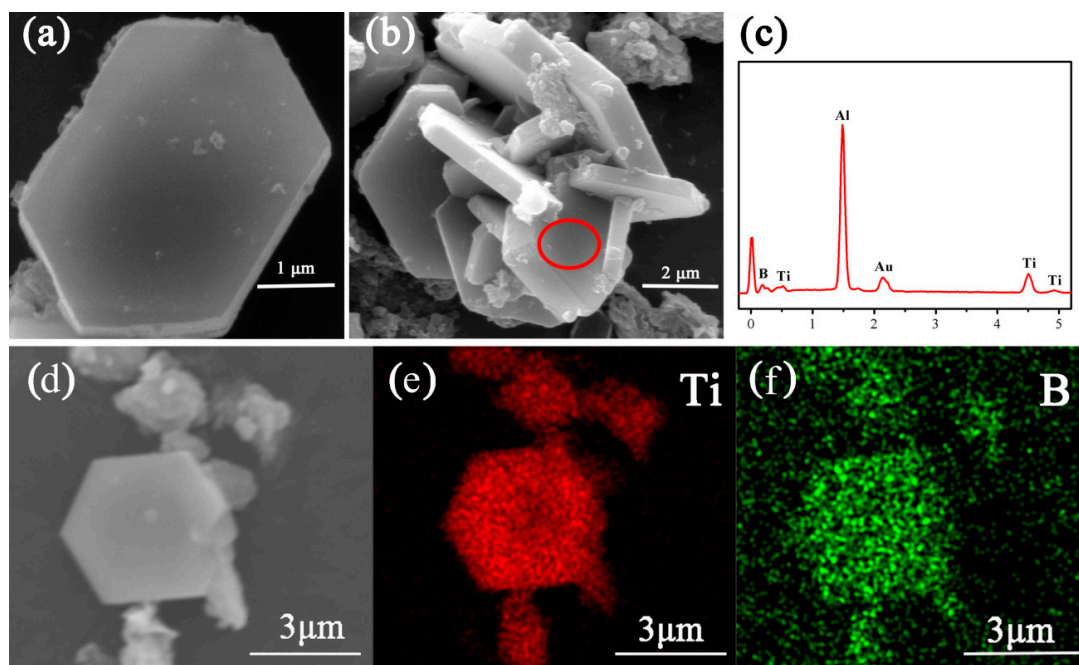
Figure 5. SEM images of (**a**) monodispersed TiB_2 microplatelet and (**b**) interlaced TiB_2 microplatelets, (**c**) corresponding EDS results of TiB_2 microplatelets, (**d**) a lower magnification SEM image with EDS mappings of (**e**) Ti element and (**f**) B element prepared *via* MSM-BCTR at 1200 °C for 20 min. (Au and Al peaks in Figure 5b were from the gold coating and aluminum foil used for enhancing electrical conductivity of the powder sample.)

TEM (Figure 6a) further reveals the high crystalline extent of as-prepared TiB_2 particles and their hexagonal plate-like morphology. SAED (Figure 5b) taken from a well-defined TiB_2 microplatelet (indicated by the red circle in Figure 5a) verifies its single-crystalline nature, and its anisotropic structure formed from the preferential growth along the [010] direction. The high-resolution TEM image shown in Figure 5c further reveals that the hexagonal micro-platelet had well-aligned lattice fringes with a constant interplanar spacing of 0.262 nm, which was in good agreement with the (100) interplanar distance of TiB_2 crystal [24]. On the basis of these results, it could be considered that the TiB_2 powders prepared *via* MSM-BCTR exhibited single-crystalline nature, uniform hexagonal plate-like morphology as well as great potential in reinforcing their bulk counterparts. Such results and the much reduced synthesis temperature and dwelling time described and discussed above, were mainly attributed to the synergistic effects of microwave heating and molten salt medium.
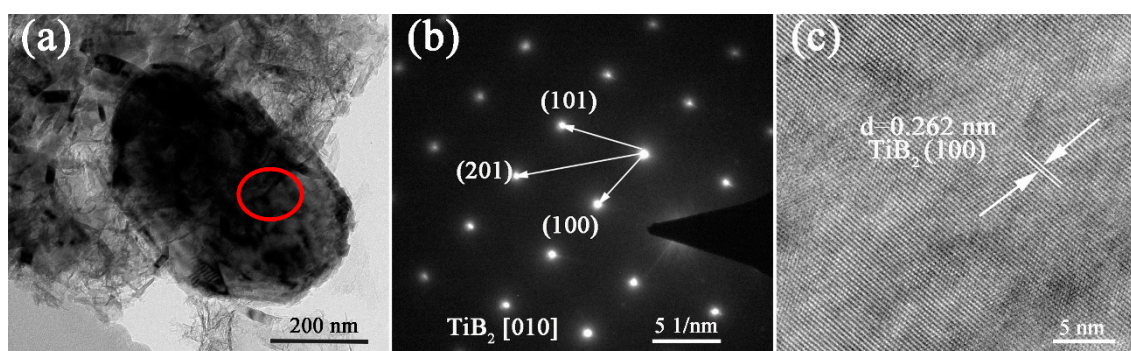
Figure 6. (**a**) Low-magnification TEM image and (**b**) SAED pattern of a representative TiB_2 microplatelet in the sample prepared *via* MSM-BCTR at 1200 °C for 20 min, and (**c**) high-resolution TEM image taken in the area defined by the red circle in (**a**).

4. Conclusions

Phase pure TiB_2 microplatelets were successfully prepared from inexpensive raw material powders of TiO_2, B_4C and C *via* MSM-BCTR treatments in KCl-NaCl medium at either 1150 °C/60 min or 1200 °C/20 min. Such synthetic conditions were considerably milder than that required by the conventional BCTR routes using the identical reducing agent. As-synthesized TiB_2 powders were single-crystalline, and exhibited well-defined hexagonal plate-like morphology with great potential in toughening their bulk counterparts. The achievement in high-efficiency, energy-saving and low-cost preparation of high-quality TiB_2 microplatelets was attributable to the synergistic effects of microwave heating and molten-salt medium.

References

1. Guo, W.; Zhang, G.; You, Y.; Wu, S.; Lin, H. TiB_2 powders synthesis by borothermal reduction in TiO_2 under vacuum. *J. Am. Ceram. Soc.* **2014**, *97*, 1359–1362. [CrossRef]
2. Zhang, G.; Ni, D.; Zou, J.; Liu, H.; Wu, W.; Liu, J.; Suzuki, T.S.; Sakka, Y. Inherent anisotropy in transition metal diborides and microstructure/property tailoring in ultra-high temperature ceramics-A review. *J. Eur. Ceram. Soc.* **2018**, *38*, 371–389. [CrossRef]

3. Fahrenholtz, W.; Hilmas, G.; Talmy, I.; Zaykoski, J. Refractory diborides of Zirconium and Hafnium. *J. Am. Ceram. Soc.* **2007**, *90*, 1347–1364. [CrossRef]

4. Basu, B.; Raju, G.; Suri, A. Processing and properties of monolithic TiB_2 based materials. *Int. Mater. Rev.* **2013**, *51*, 352–374. [CrossRef]

5. Chlup, Z.; Bača, Ľ.; Halasová, M.; Neubauer, E.; Hadraba, H.; Stelzer, N.; Roupcová, P. Effect of metallic dopants on the microstructure and mechanical properties of TiB_2. *J. Eur. Ceram. Soc.* **2015**, *35*, 2745–2754. [CrossRef]

6. Taranenko, V.I.; Zarutskii, I.V.; Shapoval, V.I.; Matiasovsk, M.; Matiasovsk, K. Mechanism of the cathode process in the electrochemical synthesis of TiB2 in molten salts-II. Chloride-Fluoride Electrolytes. *Electrochim. Acta* **1992**, *37*, 263–268. [CrossRef]

7. Sahoo, S.; Singh, S.K. Synthesis of TiB_2 by extended arc thermal plasma. *Ceram. Int.* **2017**, *43*, 15561–15566. [CrossRef]

8. Tabriz, B.N.; Adhami, T.; Kahrizsangi, R.E. Effect of processing parameters on the formation of TiB_2 nanopowder by mechanically induced self-sustaining reaction. *Ceram. Int.* **2014**, *40*, 7345–7354. [CrossRef]

9. Kang, S.H.; Kim, D.J. Synthesis of nano-titanium diboride powders by carbothermal reduction. *J. Eur. Ceram. Soc.* **2007**, *27*, 715–718. [CrossRef]

10. Yu, J.; Ma, L.; Zhang, Y.; Gong, H.; Zhou, L. Synthesis of TiB_2 powders *via* carbothermal reduction of TiO_2, HBO_2 and carbon black. *Ceram. Int.* **2016**, *42*, 5512–5516. [CrossRef]

11. Derin, B.; Kurtoglu, K.; Sahin, F.C.; Yucel, O. Thermochemical modeling and experimental studies on the formation of TiB_2 through carbothermic synthesis from TiO_2 and B_2O_3 or B_4C. *Ceram. Int.* **2017**, *43*, 10975–10982. [CrossRef]

12. Yu, J.; Ma, L.; Abbas, A.; Zhang, Y.; Gong, H.; Wang, X.; Zhou, L.; Liu, H. Carbothermal reduction synthesis of TiB_2 ultrafine powders. *Ceram. Int.* **2016**, *42*, 3916–3920. [CrossRef]

13. Moradi, V.; Nikzad, L.; Mobasherpour, I.; Razavi, M. Low temperature synthesis of titanium diboride by carbothermal method. *Ceram. Int.* **2018**, *44*, 19421–19426. [CrossRef]

14. Liu, D.; Chu, Y.; Jing, S.; Ye, B.; Zhou, X. Low-temperature synthesis of ultrafine TiB_2 nanopowders by molten-salt assisted borothermal reduction. *J. Am. Ceram. Soc.* **2018**, *101*, 5299–5303. [CrossRef]

15. Welham, N.J. Formation of nanometric TiB_2 from TiO_2. *J. Am. Ceram. Soc.* **2000**, *83*, 1290–1292. [CrossRef]

16. Bao, K.; Wen, Y.; Khangkhamano, M.; Zhang, S. Low-temperature preparation of titanium diboride fine powder *via* magnesiothermic reduction in molten salt. *J. Am. Ceram. Soc.* **2017**, *100*, 2266–2272. [CrossRef]

17. Tan, C.; Liu, J.; Zhang, H.; Wang, J.; Li, S.; Song, J.; Zhang, Y.; Zhang, S. Low-temperature synthesis of 2H-SiC powders *via* molten-salt-mediated magnesiothermic reduction. *Ceram. Int.* **2017**, *43*, 2431–2437. [CrossRef]

18. Zhang, S.; Khangkhamano, M.; Zhang, H.; Yeprem, H.A. Novel synthesis of ZrB_2 powder *via* molten-salt-mediated magnesiothermic reduction. *J. Am. Ceram. Soc.* **2014**, *97*, 1686–1688. [CrossRef]

19. Subramanian, C.; Murthy, T.S.R.C.; Suri, A.K. Synthesis and consolidation of titanium diboride. *Int. J. Refract. Met. Hard Mater.* **2007**, *25*, 345–350. [CrossRef]

20. Wu, J.; Niu, B.; Zhang, F.; Lei, L.; Zhang, J.; Ren, L.; Wang, W.; Fu, Z. Effect of titanium diboride on the homogeneity of boron carbide ceramic by flash spark plasma sintering. *Ceram. Int.* **2018**, *44*, 15323–15330. [CrossRef]

21. Ma, L.; Yu, J.; Guo, X.; Xie, B.; Gong, H.; Zhang, Y.; Zhai, Y.; Wu, X. Preparation and sintering of ultrafine TiB_2 powders. *Ceram. Int.* **2018**, *44*, 4491–4495. [CrossRef]

22. Rabiezadeh, A.; Hadian, A.M.; Ataie, A. Synthesis and sintering of TiB_2 nanoparticles. *Ceram. Int.* **2014**, *40*, 15775–15782. [CrossRef]

23. Zhang, H.; Li, F. Preparation and microstructure evolution of diboride ultrafine powder by sol–gel and microwave carbothermal reduction method. *J. Sol-Gel Sci. Technol.* **2007**, *45*, 205–211. [CrossRef]

24. Javadi, A.; Pan, S.; Cao, C.; Yao, G.; Li, X. Facile synthesis of 10 nm surface clean TiB_2 nanoparticles. *Mater. Lett.* **2018**, *229*, 107–110. [CrossRef]

25. Wei, T.; Liu, Z.; Ren, D.; Deng, X.; Deng, Q.; Huang, Q.; Ran, S. Low-temperature synthesis of TaB_2 nanorods by molten-salt assisted borothermal reduction. *J. Am. Ceram. Soc.* **2018**, *101*, 45–49. [CrossRef]

26. Danko, G.A.; Silberglitt, R.; Colombo, P.; Pippel, E.; Woltersdorf, J. Comparison of microwave hybrid and conventional heating of preceramic polymers to form silicon carbide and silicon oxycarbideceramics. *J. Am. Ceram. Soc.* **2004**, *83*, 1617–1625. [CrossRef]

27. Gordon, J.; Kazemian, H.; Rohani, S. Rapid and efficient crystallization of MIL-53(Fe) by ultrasound and microwave irradiation. *Microporous Mesoporous Mater.* **2012**, *162*, 36–43. [CrossRef]

28. Liu, H.; Xiang, K.; Yang, B.; Yang, S.; Chai, L. Microwave intensified synthesis of regular shaped sodium bisulfate crystal. *Chem. Eng. Process. Process Intensif.* **2015**, *95*, 208–213. [CrossRef]

29. Liu, J.; Huang, Z.; Huo, C.; Li, F.; Zhang, H.; Zhang, S. Low-temperature rapid synthesis of rod-like ZrB_2 powders by molten-salt and microwave co-assisted carbothermal reduction. *J. Am. Ceram. Soc.* **2016**, *99*, 2895–2898. [CrossRef]

30. Zeng, Y.; Liang, F.; Liu, J.; Zhang, J.; Zhang, H.; Zhang, S. Highly efficient and low-temperature preparation of plate-like ZrB_2-SiC powders by a molten-salt and microwave-modified boro/carbothermal reduction method. *Materials* **2018**, *11*, 1811. [CrossRef]